USE OF PARAMAGNETIC-RESONANCE TECHNIQUES IN THE STUDY OF ATOMIC-OXYGEN RECOMBINATIONS

S. KRONGELB and M. W. P. STRANDBERG

TECHNICAL REPORT 291
MAY 20, 1959

MASSACHUSETTS INSTITUTE OF TECHNOLOGY
RESEARCH LABORATORY OF ELECTRONICS
CAMBRIDGE, MASSACHUSETTS

Reprinted from THE JOURNAL OF CHEMICAL PHYSICS, Vol. 31, No. 5, pp. 1196–1210, November, 1959

The Research Laboratory of Electronics is an interdepartmental laboratory of the Department of Electrical Engineering and the Department of Physics.

The research reported in this document was made possible in part by support extended the Massachusetts Institute of Technology, Research Laboratory of Electronics, jointly by the U. S. Army (Signal Corps), the U. S. Navy (Office of Naval Research), and the U. S. Air Force (Office of Scientific Research, Air Research and Development Command), under Signal Corps Contract DA36-039-sc-78108, Department of the Army Task 3-99-20-001 and Project 3-99-00-000.

Reprinted from the JOURNAL OF CHEMICAL PHYSICS, Vol. 31, No. 5, 1196-1210, November, 1959
Printed in U. S. A.

Use of Paramagnetic-Resonance Techniques in the Study of Atomic Oxygen Recombinations*

S. KRONGELB† AND M. W. P. STRANDBERG

Department of Physics and Research Laboratory of Electronics, Massachusetts Institute of Technology, Cambridge, Massachusetts

(Received April 27, 1959)

A method of making measurements of atomic recombination times with the use of a paramagnetic-resonance spectrometer and its advantages are described. The theory of the paramagnetic-resonance spectrometer applied to these measurements is presented. Methods for using both diffusion and flow systems for determining surface and volume recombination coefficients are analyzed. The operation of the system that was used is illustrated for atomic oxygen recombination. The surface recombination coefficient for oxygen atoms on a quartz surface is shown to be 3.2×10^{-4} per collision, and the second-order volume recombination coefficient was less accurately determined as 5×10^{15} cm^6 mole^{-2} sec^{-1}. The measurement of the diffusion coefficient of atomic oxygen is described. The possible application of these methods to further study of reaction rates is discussed.

I. INTRODUCTION

RECOMBINATION, particularly of oxygen atoms, plays a role in many commonplace phenomena. Any process that results in sufficiently high temperatures to produce dissociation is also affected by recombination. Thus, our description of the energy distribution and products of such varied phenomena as gas discharges, dynamite blasts, or hot flames cannot be complete without considering recombination processes. The advent of guided missiles has accelerated interest in recombination, since the heat generated upon re-entry into the atmosphere is sufficient to produce dissociation of the gases at the nose cone.

In spite of this extensive interest in oxygen recombination, our quantitive understanding of this reaction has been restricted by the available experimental techniques. The basic problem of measuring recombination rates is that of observing atomic oxygen concentration as a function of time (or of some variable related to time). In most of the recombination work heretofore reported,[1-4] the concentration was determined by introducing a metal probe into the system and measuring the temperature rise that resulted from the heating by oxygen atoms recombining on the probe. This method has disadvantages: (1) It is slow because the probe must be allowed to reach thermal equilibrium. (2) The accuracy is limited by temperature measurement, and by the fact that small variations in surface contamination of the probe can strongly affect the recombination rate. (3) The presence of the probe in the system can be a disturbing influence to the recombination process that is being studied. In this paper we indicate how atomic oxygen paramagnetism can be utilized to provide convenient and accurate means of measuring oxygen concentration in recombination studies. Before presenting our techniques and results, a brief description of recombination and of the paramagnetic properties of atomic oxygen is given.

The recombination reaction is basically a three-body reaction that can be characterized chemically by the equation

$$O+O+M\rightarrow O_2+M.$$

The third body is designated by M and is considered as playing the role of a catalyst. Physically, its presence is required to satisfy conservation of energy and of momentum.

Recombination problems can be classified according to the nature of the third body. The first class can be called surface recombination and refers, as its name indicates, to situations in which the oxygen atoms meet at the surface of the reaction vessel. The presence of the wall enables conservation of energy and momentum. Wall recombinations are best characterized by an efficiency coefficient γ which is defined as the fraction of the atoms striking the surface which becomes molecules. It is known that the value of γ depends on the surface material.

The second class of recombination can be called volume recombination and includes the case in which the third body is an atom or molecule. In our experiments, the concentration of atomic oxygen is comparatively small; hence a three-body collision involving three oxygen atoms is unlikely, and the volume reaction has an oxygen molecule as the third body. The third body need not be oxygen in any form. It is hoped that the techniques of these experiments will be applied to the study of the effects of other gases that may be introduced into the system as the third body.

* This work, which was supported in part by the U. S. Army (Signal Corps), the U. S. Air Force (Office of Scientific Research, Air Research and Development Command), and the U. S. Navy (Office of Naval Research), is based on a Ph.D. thesis submitted to the Department of Physics, M.I.T., June, 1958.

† Now with IBM Research Center, Yorktown Heights, New York.

[1] I. Amdur and A. L. Robinson, J. Am. Chem. Soc. **55**, 1395 (1933).

[2] W. V. Smith, J. Chem. Phys. **11**, 110 (1943).

[3] J. W. Linnett and D. G. H. Marsden, Proc. Roy. Soc. (London) **A234**, 489 (1956).

[4] J. W. Linnett and D. G. H. Marsden, Proc. Roy. Soc. (London) **A234**, 504 (1956).

II. ATOMIC OXYGEN PARAMAGNETISM

Resonance Properties

The property of atomic oxygen which makes the study of recombination reactions possible is its strong paramagnetic-resonance absorption. By allowing the reaction to take place in the cavity of a paramagnetic-resonance spectrometer, we can follow the course of the reaction by observing the intensity of the absorption. The interpretation of the data then depends on understanding the paramagnetic properties of oxygen.

Paramagnetic-resonance absorption in atomic oxygen was first observed by Rawson and Beringer,[5] and its theoretical implications were discussed by Abragam and Van Vleck.[6] Interaction with microwave radiation arises from transitions between the Zeeman energy levels. The simple resonance condition is $h\nu = g\beta H$, where ν is the microwave frequency, g is the Landé g-factor, H is the applied magnetic field, h is Planck's constant, and β refers to the Bohr magneton. The transitions that contribute to the paramagnetic absorption, taken from Abragam and Van Vleck, are shown in Fig. 1. In addition to the $^3P_1$ states shown, ^1D and ^1S states lying 15 867.7 cm^{-1} and 33 792.4 cm^{-1} above the $^3P_2$ level are also possible. However, these states are sparsely populated because of the Boltzmann factor and thus do not contribute to the absorption. It should be noted in this connection that, although the atomic states are produced by oxygen flowing through a microwave discharge, the gas just beyond the discharge is at room temperature. This temperature measurement was made by comparing the relative intensity of the $^3P_1$ and $^3P_2$ transitions (see Fig. 2).

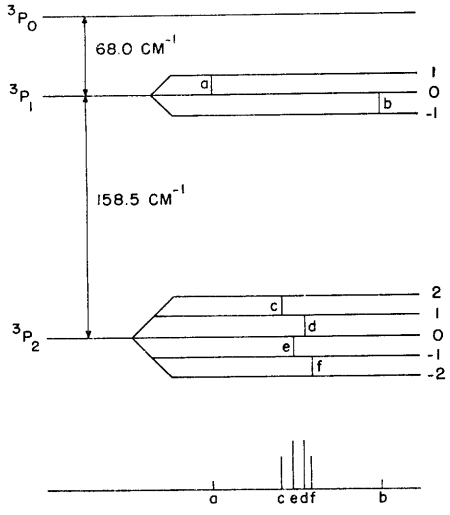

FIG. 1. Energy levels and transitions of atomic oxygen in a magnetic field.

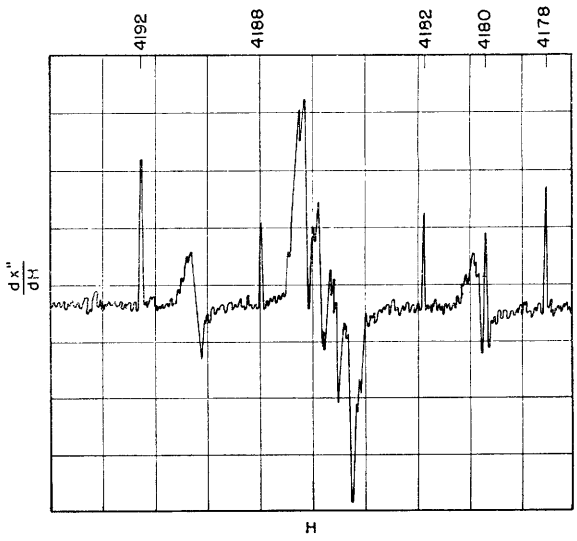

FIG. 2. Atomic oxygen resonance showing fine structure. The numbers refer to field measurements in gauss.

Relative Concentration Measurements

The quantitive description of the absorption is conveniently given in terms of χ'', the imaginary part of the susceptibility. The usual analysis[7] for pressure-broadened transitions in the microwave region gives for the Jm, $J'm'$ transition

$$\chi''_{Jm,J'm'} = N\frac{\omega}{kT}\frac{\exp(-E_{Jm}/kT)}{Z}\,|(\mu_r)_{Jm,J'm'}|^2 f(\omega-\omega_0), \tag{1}$$

where N is the number of atoms in the system per cubic centimeter; ω is the angular frequency of the transition; E_{Jm} is the energy of the Jm state; Z is the partition sum; $|(\mu_r)_{Jm,J'm'}|^2$ is the absolute square of the transition matrix element in the direction of the rf field; and $f(\omega-\omega_0)$ is the shape factor that gives the effect of pressure broadening. In applying Eq. (1) to atomic oxygen we must remember that, although the individual transitions can be resolved as shown in Fig. 2, the conditions of recombination experiments result in incomplete resolution. The total absorption is thus obtained by summing over the individual transitions. We obtain

$$\chi''(\omega) = (N/Z)(\omega/kT)\sum_i \exp(-E_{Jm}{}^{(i)}/kT) \cdot |(\mu_r)^{(i)}_{Jm,J'm'}|^2 f(\omega-\omega_0{}^{(i)}), \tag{2}$$

in which the superscript (i) denotes the particular transition.

To evaluate the matrix element, the component of $\boldsymbol{\mu}$ in the direction of the rf field, it is convenient to ex-

[5] E. B. Rawson and R. Beringer, Phys. Rev. (Letters) **88**, 677 (1952).

[6] A. Abragam and J. H. Van Vleck, Phys. Rev. **92**, 1448 (1953).

[7] J. H. Van Vleck and V. F. Weisskopf, Revs. Modern Phys. **17**, 227 (1945).

pand $\mathbf{H}_{rf}$ and $\mathfrak{y}$ in terms of $H_\pm$ and $\mu_\pm$. For $H_\pm=(H_x\mp iH_y)/\sqrt{2}$ and $\mu_\pm=(\mu_x\pm i\mu_y)$, we have

$$\mathbf{H}_{rf}\cdot\mathfrak{y}_{Jm,J'm'}=H_+(\mu_+)/\sqrt{2}+H_-(\mu_-)/\sqrt{2}+H_z\mu_z.$$

The convenience of this expansion arises from the fact that the requirements for nonvanishing μ_+, μ_-, and μ_z are $\Delta m=+1$, -1, and 0, respectively. Thus only one term contributes to the matrix element for any given transition. As an illustration, for $\Delta m=+1$, we have

$$|(\mu)_{Jm,J'm'}|^2=(f_+/2)\,|(\mu_+)_{Jm,J'm'}|^2, \qquad (3)$$

where

$$f_+=\int|H_+|^2dV_{\text{sample}}/\int|H|^2dV_{\text{cavity}}.$$

Matrix elements for $\Delta m=0$ and $\Delta m=-1$ transitions can be similarly evaluated.

The transitions that we are discussing take place between energy levels of finite width, so that a shape factor $f(\omega-\omega_0)$ has to be introduced. For a gas at millimeter pressures, the width results from molecular collisions, and we have

$$f(\omega-\omega_0)=\tau^{-1}/[(\omega-\omega_0)^2+\tau^{-2}],$$

where $\tau^{-1}=2\pi\Delta\nu=\Delta\omega$. Since the usual paramagnetic-resonance experiment is performed by keeping the frequency constant and varying the field, it is necessary to transform $f(\omega-\omega_0)$. This is done by using the relation

$$\omega=\omega_\alpha+(d\omega/dH)(H-H_0),$$

which is valid in the region of resonance, and in which H is the resonant field at angular frequency ω_0. If we define g_{eff} as

$$g_{\text{eff}}=(\hbar/\beta)(d\omega/dH),$$

we have

$$f(\omega-\omega_0)=\frac{\hbar}{g_{\text{eff}}\beta}\frac{\Delta H}{(H-H_0)^2+(\Delta H)^2}=\frac{\hbar}{g_{\text{eff}}\beta}f(H-H_0). \qquad (4)$$

(For simple cases, $\hbar\omega=g\beta H$, hence g_{eff} is the Landé g factor.)

The total absorption for an observed line is defined by the integral of Eq. (2) [transformed by Eq. (4)] with respect to H. Since the integral of $f(H-H_0)$ over all H is equal to $\pi/2$, the total absorption for a particular line is dependent on N and other constant factors. Although recombination experiments could be performed by considering the total absorption, the analysis of data would be greatly simplified if the integration could be avoided. We shall therefore consider under what conditions $f(H-H_0)$ remains unchanged; that is, under what conditions the absorption at a fixed value of H is a function of N only. [Strictly speaking, the line shape for the incompletely resolved transition that we observe is not given simply by $f(H-H_0)$. The assumption that $f(H-H_0)$ does, to some degree of accuracy, describe our line is based on the fact that 80 percent of the intensity arises from nearly coincident transitions, so that $f(H-H_0)$ can be taken out of the summation in Eq. (2).]

For the range of pressures in which our experiments are performed, collision-broadening theory applies. The parameter $1/\tau$ is the average collision frequency for a molecule, expressed by

$$1/\tau=\pi b^2\bar{v}_{\text{rel}}N,$$

where b is the effective diameter of the molecule, $\bar{v}_{\text{rel}}$ is the average relative velocity, and N is the number of molecules per unit volume. This expression is correct for a gas containing one type of molecule only, but the extension to a mixture can be readily made. For instance, the number of collisions which a molecule of type b makes in a mixture containing molecules a and b is

$$(1/\tau)_b=\pi b^2\bar{v}_{bb}N_b+\pi(\sigma_{ab})^2\bar{v}_{ab}N_a. \qquad (5)$$

Here N_a and N_b are the concentrations of molecules a and b, respectively; $\bar{v}_{bb}$ is the average relative velocity between two molecules of type b; $\bar{v}_{ab}$ is the velocity of b relative to a; and σ_{ab} is the effective collision diameter for the mixed collision.

Our recombination data are obtained by looking at the oxygen atoms in a mixture of atomic and molecular oxygen. Line width is thus governed by Eq. (5), and depends, in general, upon the relative concentrations of the two gases, as well as the total pressure. Certain simplifications, however, are possible for our experimental conditions, since the total pressure for a given run (i.e., N_a+N_b) is constant. Furthermore, N_b, the atomic concentration, is usually less than 10 percent of N_a+N_b, and therefore we can write

$$N_b=\alpha(N_a+N_b)=\alpha N,$$

where α is less than 0.1. Then $N_a=N(1-\alpha)$, and Eq. (5) becomes

$$(1/\tau_b)=[\pi b^2\bar{v}_{bb}\alpha+\pi(\sigma_{ab})^2\bar{v}_{ab}(1-\alpha)]N$$
$$=[\pi b^2\bar{v}_{bb}-\pi(\sigma_{ab})^2\bar{v}_{ab}]\alpha N+[\pi(\sigma_{ab})^2\bar{v}_{ab}]N.$$

The second term is a constant. The first term varies with the relative concentration α; but α does not exceed 0.1, so that unless the bracketed part of the first term is much larger than that in the second term, $1/\tau$ is essentially constant. This constancy has been verified experimentally within one-tenth of a gauss for the full range of α of our experiments.

It should be pointed out that the constancy of τ, although it seems plausible from our discussion, cannot be assumed. Both σ_{ab} and b depend on the type of interaction between the two molecules, and there is no assurance that $\sigma_{ab}^2\bar{v}_{ab}$ will be comparable to $b^2\bar{v}_{bb}$. The constancy of τ whould be empirically reconsidered if other gases are introduced.

The determination of atomic oxygen concentration at constant total pressure is now relatively simple. We must remember that the paramagnetic-resonance spectrometer gives an output that is proportional to the derivative of χ''; that is, the shape factor is $df(H-H_0)/dH$ rather than $f(H-H_0)$. It is then convenient to use the maximum of the derivative as our measure of concentration. The functional constancy of $f(H-H_0)$ implies, of course, the same invariance for the derivative. Thus the maximum of the derivative is indeed proportional to the concentration.

Absolute Concentration Measurements

The discussion already given provides all the information we need for making relative concentration measurements. But for certain purposes (e.g., evaluation of reaction rate constants other than first-order), it is necessary to know the absolute concentration of the reactants. This measurement can, in principle, be made by evaluating certain constants of the apparatus. The difficulty of such a procedure, however, precludes its use with appreciable accuracy and suggests an alternative method wherein the atomic oxygen absorption is compared with absorption by a known concentration of oxygen molecules. The problem then reduces to a relative concentration measurement, and we need know only the relative magnitude of χ'' for atomic and for molecular oxygen.

For atomic oxygen, χ'' is given by Eq. (2), which we can write more explicitly by evaluating the matrix elements. We are particularly interested in the $\Delta m=+1$ transitions, and hence, according to Eq. (3), in the matrix elements of μ_+, which are given[8] by

$$(\alpha' J, m+1 \mid \mu_+ \mid \alpha, J, m) = C(\alpha' J, \alpha J)[(J-m)(J+m+1)]^{\frac{1}{2}}. \quad (6)$$

The coefficient $C(\alpha' J, \alpha J)$ is found by considering the matrix element

$$(\alpha' Jm \mid \mu_z \mid \alpha Jm) = C(\alpha' J, \alpha J)m.$$

For $\mu_z=\beta(g_L\mathbf{L}+g_s\mathbf{S})$ this element is just the one involved in calculating the Zeeman-energy splitting. Thus, we see by inspection that $C(\alpha' J, \alpha J)$ is β times the Landé g factor.

In comparing atomic and molecular oxygen intensities we must work with the integrated intensities. By integrating Eq. (2), we obtain

$$\int \chi_O'' dH = N_O(\pi/2)(\hbar\omega/g\beta kT)(1/Z)\sum_{Jm} \exp(-E_{Jm}/kT)\,|(\mu_r)_{Jm,J'm'}|^2.$$

If we define N_O as the density of oxygen atoms in the ^3P states (the only states that are appreciably populated), the partition sum is evaluated by summing over the energy levels in Fig. 1. For this purpose, we may consider the magnetic sublevels as degenerate; therefore at 300°K, with the aid of Eqs. (3) and (6), we obtain

$$\int \chi_O'' dH = N_O[(\pi/2)(\hbar\omega/\beta kT)](f_+/g)(3.65)\beta^2. \quad (7)$$

The molecular oxygen absorption can be calculated by using the data of Tinkham and Strandberg.[9] Since the molecular lines are completely resolved, we use Eq. (1) which, in integrated form, becomes

$$\int \chi_{O(mol)}'' dH = N_{O(mol)}\left(\frac{\pi}{2}\frac{\hbar\omega}{\beta kT}\right)\frac{\exp(-E_{Jm}/kT)}{Z}\cdot\frac{|(\mu_r)_{Jm,J'm'}|^2}{g_{eff}}. \quad (8)$$

The partition sum, Z, is approximated by its classical value $3kT/2B$ when $B=43\,102$ mc. The matrix element for $\Delta m=\pm 1$ transitions is, as in Eq. (3),

$$|(\mu_r)_{Jm,J'm'}|^2=(f_\pm/2)\,|(\mu_\pm)_{Jm,J'm'}|^2.$$

For molecular oxygen, μ, in Tinkham and Strandberg's notation is, $g_s\beta\mathbf{S}$. Thus, we are concerned with the matrix element

$$(Jm \mid S_\pm \mid J'm') = 4(Jm \mid S_x \mid J'm').$$

By inserting this relation in Eq. (8), and dividing by Eq. (7), we obtain

$$\frac{N_O}{N_{O(mol)}}=\frac{g_O}{g_{eff(mol)}}\cdot\frac{[4\,|(Jm \mid S_x \mid J'm')|^2\exp(-E_{Jm}/kT)]}{394}\cdot\frac{\int\chi_O''dH}{\int\chi_{O(mol)}''dH}. \quad (9)$$

The quantity in brackets is calculated, or derived empirically, by Tinkham and Strandberg for several transitions. The transition that we found most convenient was the $K=5$, $J=4\rightarrow 6$, $M=1\rightarrow 2$ for which the bracketed value is 0.37, and $g_{eff}=1.34$. For atomic oxygen, $g=1.5$, so that

$$\frac{N_O}{N_{O(mol)}}=1.05\times 10^{-3}\frac{\int\chi_O''dH}{\int\chi_{O(mol)}''dH}. \quad (10)$$

Equation (10) or an equivalent expression—if we do not use this particular molecular oxygen transition for

[8] E. Feenberg and G. E. Pake, *Notes on the Quantum Theory of Angular Momentum* (Addison-Wesley Publishing Company, Inc., Reading, Massachusetts, 1953), p. 36f.

[9] M. Tinkham and M. W. P. Strandberg, Phys. Rev. **97**, 937 (1955).

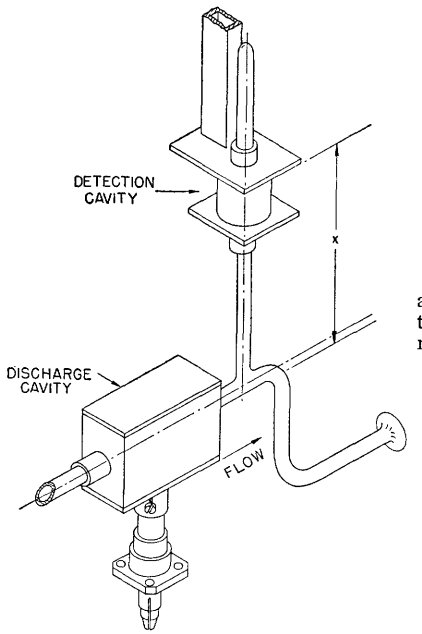

FIG. 3. Detection and discharge cavities for side-arm method.

the comparison—is directly applicable to the determination of atomic oxygen concentration. A method for evaluating the integrals directly from the output of the spectrometer is given in Appendix B.

III. ANALYSIS OF RECOMBINATION METHODS

Side-Arm Method

The most direct method for observing recombination is to create the oxygen atoms by a discharge inside the paramagnetic-resonance spectrometer cavity, shut off the discharge, and observe the output of the spectrometer as a function of time. Although no data were obtained by this method because of interaction of the discharge with the spectrometer, the difficulties do not seem insurmountable, and the direct method should not be overlooked as a worthwhile technique. This method may, in fact, provide a good means for observing volume recombination. In our work we observed recombination by adapting two techniques that have been used previously for reaction studies. These are the side-arm method of Smith[2] which has been used to study surface recombination of hydrogen, and the flow system, an old stand-by in reaction studies.

Our adaptation of the side-arm method is illustrated in Fig. 3; it consists of a flow tube with a discharge arranged to create atomic oxygen at a point near the beginning of the tube. A closed tube, the side arm, is attached to the flow tube at a point downstream from the discharge. This junction functions as constant-concentration atomic oxygen source for the side arm. The balance between atoms diffusing from this source into the side arm and the loss of atoms by recombination gives rise to the concentration gradient along the side arm which can be related to the recombination mechanism. Various possible recombination mechanisms are:

(1) Surface recombination that is proportional to the first power of the atomic oxygen concentration.

(2) Surface recombination that requires that two oxygen atoms meet simultaneously at the surface; i.e., a second-order reaction.

(3) Recombination, also of second-order, by the reaction

$$O+O+O_2\rightarrow O_2+O_2.$$

(4) Third-order recombination according to the reaction

$$O+O+O\rightarrow O_2+O.$$

(5) Losses involving the formation of ozone or reactions with impurities in the oxygen.

It will be seen that mechanism (1) governs surface recombination, and that (3) is the most probable volume process.

The differential equation governing the concentration in the side arm when these two loss mechanisms predominate has been derived by Smith[2]:

$$d^2C/dx^2=\gamma(\bar{v}/2RD)C+(k_2[M]/D)C^2, \qquad (11)$$

where C = concentration of atomic oxygen; x = distance down the side arm; $\bar{v}$ = average thermal velocity of O atoms; R = radius of side arm; D = diffusion coefficient for oxygen atoms; $[M]$ = concentration of the third body in the volume recombination (in this case O_2); γ = fraction of the atoms striking the surface which recombine; and k_2 = second-order rate constant for the reaction $dC/dt=-k_2C^2[M]$. For convenience, we rewrite Eq. (11) as

$$d^2C/dx^2=\alpha^2C+\beta^2C^2, \qquad (12)$$

where α and β are defined by the coefficients of C and C^2 in Eq. (11).

For the conditions of many of our experiments, surface recombination predominates to such an extent that β may be set equal to zero. Then Eq. (12) becomes

$$d^2C/dx^2=\alpha^2C, \qquad (13)$$

which has for a solution

$$C=Ae^{-\alpha x}+Be^{+\alpha x}. \qquad (14)$$

The second term may be considered as representing atoms reflected from the closed end of the tube. In general, the concentration at this end will be so small that B is zero, and we have

$$C=C_0\,e^{-\alpha x}, \qquad (15)$$

where C_0 is the concentration at $x=0$.

Equation (12) can also be solved with $\alpha=0$, as well as with both α and β not equal to zero. The former

case corresponds to pure second-order recombination, and has for a solution

$$C(x)=C_0/[1+\beta x(C_0/6)^{\frac{1}{2}}]^2. \quad (16)$$

For our experimental conditions, pure volume recombination is never observed in the side arm. However, by a suitable definition of β, Eq. (15) can be taken to represent second-order surface recombination. That surface recombination is a first-order process will be shown by the fact that the data fit Eq. (14) and not Eq. (16).

If both surface and volume effects occur simultaneously, neither α nor β vanish, and the solution is given by

$$\frac{[1+(\beta/\alpha)^2C]^{\frac{1}{2}}-1}{[1+(\beta/\alpha)^2C]^{\frac{1}{2}}+1}=\frac{[1+(\beta/\alpha)^2C_0]^{\frac{1}{2}}-1}{[1+(\beta/\alpha)^2C_0]^{\frac{1}{2}}+1}e^{(-\alpha x)}. \quad (17)$$

Data corresponding to this solution (that is, with surface and volume recombination of comparable magnitudes) have not been observed. Equation (17) is useful, however, for checking whether there are any departures from pure first-order effects and estimating the magnitude of second-order reactions.

In developing the equation for the side arm we have made two assumptions: (1) that diffusion theory applies, and (2) that there is no radial concentration gradient. The first assumption will be valid if the mean-free path is much smaller than the diameter of the side arm. For a 1-cm side arm, this condition holds down to pressures of approximately 0.1 mm.

The assumption of no radial concentration gradients is valid if diffusion is sufficiently rapid to wipe out the gradients caused by recombination at the wall. The relaxation time for the diffusion process is given by $t=R^2/D$. All of the atoms initially contained in a length dx of the side arm, on the other hand, recombine in a time

$$t=c\pi R^2dx/\gamma(c\bar{v}/4)2\pi Rdx$$
$$=2R/\gamma\bar{v}.$$

Radial concentration gradients will be wiped out if the time for diffusion relaxation is much less than the time for recombination, for example, if $R^2/D\ll 2R/\gamma v$. At 3 mm Hg (the highest pressure used), $R^2/D=3$ msec, and $2R/\gamma v$ is approximately 0.1 sec. Thus the requirement is well satisfied.

Diffusion Coefficient Measurements

Since the side-arm experiment is based on a balance between diffusion and recombination, it is apparent that the diffusion coefficient must be known if quantitative interpretation of the data is to be given. Because of the inapplicability of conventional diffusion measurement techniques to short-lived substances, no measurements of the diffusion constant for atomic oxygen exist. We have therefore devised a means of using paramagnetic resonance to measure this diffusion constant. Our method is an extension of the side-arm technique in which we observe the nonequilibrium conditions when the source of oxygen atoms is turned on or off. If we observe atomic oxygen at some point along the side arm, the rate of approach to final equilibrium will depend on both recombination and diffusion. This measurement, combined with the observed concentration gradient along the side arm, gives us two independent pieces of data from which recombination and diffusion can be determined.

The differential equation representing the nonequilibrium situation is given by an extension of Eq. (13),

$$D\partial^2C/\partial x^2-D\alpha^2C=\partial C/\partial t. \quad (18)$$

Experimentally, it is convenient to observe the nonequilibrium state when the discharge is turned off. Therefore we desire the solution of Eq. (18), subject to the boundary conditions

$$C(x,t)=C_0\exp(-\alpha x), \quad \text{for} \quad t\leq 0,$$
$$C(0,t)=C_0, \quad \text{for} \quad t<0,$$
$$C(0,t)=0, \quad \text{for} \quad t>0.$$

This problem is analogous to that of heat flow along an imperfectly insulated rod (cf. Carslaw and Jaeger[10]) and is most conveniently handled by the method of the Laplace transform. The Laplace transform of Eq. (18) is

$$(\partial^2\bar{C}/\partial x^2)-[(D\alpha^2+p)/D]\bar{C}=-C(x,0)/D.$$

If we insert the value of $C(x,0)$ and let

$$\kappa^2=(D\alpha^2+p)/D,$$

this equation becomes

$$(\partial^2\bar{C}/\partial x^2)-\kappa^2\bar{C}=-(C_0/D)e^{-\alpha x}.$$

The general transform of the solution is, then

$$\bar{C}(x,t)=A\exp(-\kappa x)+B\exp(\kappa x)$$
$$+[C_0\exp(-\alpha x)/D(\kappa^2-\alpha^2)].$$

For the case of an infinitely long tube, $B=0$. Since $C(0,t)=0$, $\bar{C}(0,t)$ also equals 0, and we obtain

$$\bar{C}(x,t)=(C_0/p)\,e^{-\alpha x}-(C_0/p)\exp-[(D\alpha^2+p)/D]^{\frac{1}{2}}x. \quad (19)$$

The desired solution can now be obtained by finding the inverse transformation of Eq. (19) with the use of Carslaw and Jaeger's table of transforms.[10] Then we have

$$C(x,t)=C_0e^{-\alpha x}[1-\tfrac{1}{2}\operatorname{erfc}\{[x/2(Dt)^{\frac{1}{2}}]-\alpha(Dt)^{\frac{1}{2}}\}$$
$$+(e^{2\alpha x}/2)\operatorname{erfc}\{[x/2(Dt)^{\frac{1}{2}}]+\alpha(Dt)^{\frac{1}{2}}\}, \quad (20)$$

[10] H. S. Carslaw and J. C. Jaeger, *Conduction of Heat in Solids* (Clarendon Press, Oxford, 1947).

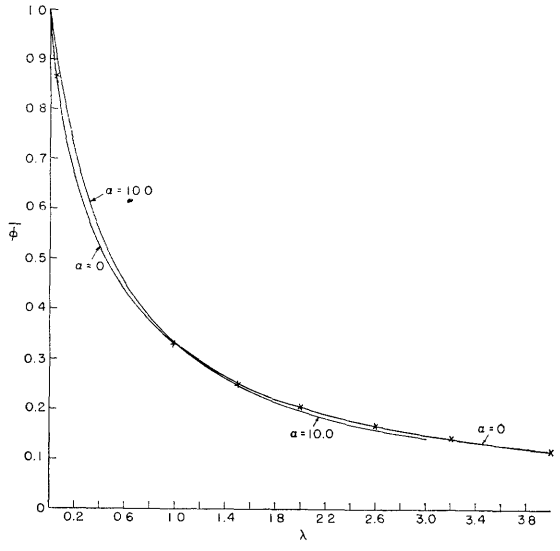

FIG. 4. Calculated $\bar{\phi}$ *vs* λ for $(1/\phi)(\partial\phi/\partial u)=0$.

where $\text{erfc}\theta=1-\text{erf}\theta$, and

$$\text{erf}\theta=2/\pi^{\frac{1}{2}}\int_0^\theta \exp(-\xi^2)d\xi.$$

D can now be determined by fitting Eq. (20) to the observed variation of C.

Flow Method

An exact analysis of a flow system results in an extremely complicated differential equation, and it is therefore necessary to treat only the most important effects. Our treatment, which is analogous to Cleland's[11] for first-order reaction, includes the ordinary Poisieulle flow and the effects of radial diffusion. Diffusion in the direction of the flow stream, caused by a concentration gradient in that direction, is neglected as being small compared with the large flow velocity. The pressure gradient, which causes the flow, and the variation in flow velocity, caused by mass changes resulting from recombinations, are also found to be negligible. With these factors neglected, the differential equation governing atomic oxygen concentration is readily found for second-order recombinations to be

$$v_z(dC/dz)=D[(\partial^2C/\partial r^2)+(1/r)(\partial C/\partial r)]-k_2[\text{M}]C^2, \tag{21}$$

where $v_z=v_0[1-(r/R)^2]$, D=diffusion constant, k_2=reaction-rate constant for the reaction $\text{O}+\text{O}+\text{M}\rightarrow\text{O}_2+\text{M}$, $[M]$=concentration of the third body, and C=concentration of atomic oxygen.

Although the solution of Eq. (21) cannot be obtained without recourse to numerical methods, the phenomena represented by this equation are simple to visualize. Because of the laminar flow, atoms near the wall travel slower than atoms near the axis of the tube. This indicates that the farther the atom is from the axis, the more chance it has to recombine during its travel down the tube. In the absence of diffusion, a radial concentration gradient is thus established. We note that this gradient results in reduced concentration at the wall, and hence reduces surface recombination. The diffusion terms that are included in Eq. (21) tend to reduce this gradient.

As mentioned, the solution of Eq. (21) requires the use of numerical techniques. It must therefore be reduced to dimensionless form. If we let

$$\phi=C/C_0,$$

$$u=r/R,$$

$$\lambda=\kappa_2C_0z/v_0,$$

and

$$\alpha=D/\kappa_2C_0R^2,$$

where

$\kappa_2=k_2[M]$, then Eq. (21) becomes

$$(1-u^2)(\partial\phi/\partial\lambda)=\alpha[\partial^2\phi/\partial u^2+(1/u)(\partial\phi/\partial u)]-\phi^2. \tag{22}$$

Equation (22) was solved by transforming it into a difference equation that was programmed for the IBM 704 computer.[12] Solutions obtained for several values of α were integrated over u to obtain the average $\bar{\phi}$ which is plotted as a function of λ in Figs. 4 and 5. In all cases the boundary conditions on ϕ were

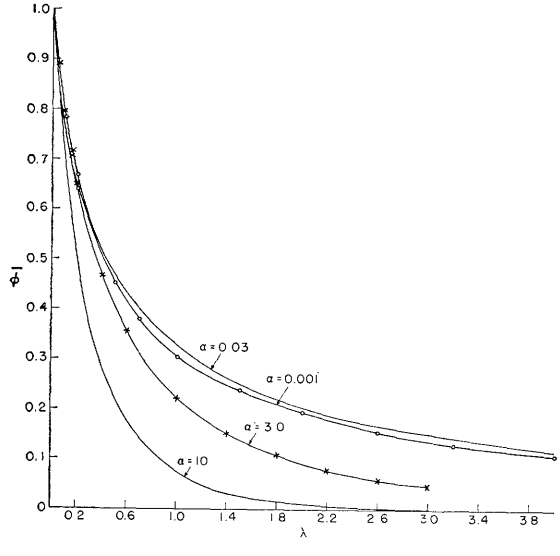

FIG. 5. Calculated $\bar{\phi}$ *vs* λ for $(1/\phi)(\partial\phi/\partial u)=-0.05$.

[11] F. A. Cleland, "Diffusion and reaction in viscous-flow tubular reactors," Ph.D. thesis, Princeton University, 1953, University Microfilms Publication No. 9400.

[12] We wish to thank Mrs. Lena Fried, who carried out the solutions of Eq. (22), and the Computation Center, MIT, which operates the IBM 704 computer.

$\phi(\lambda=0)=1$, and $\phi(\lambda\rightarrow\infty)=0$. At $u=0$, $\partial\phi/\partial u=0$ as required by symmetry. For the curves in Fig. 4, the boundary conditions at $u=1$ were $\partial\phi/\partial u=0$; that is, for no net flow of particles through the wall of the tube. In the solutions of Fig. 5 we took $(1/\phi)(\partial\phi/\partial u)=-0.05$ at $u=1$. This represented a net flow of particles into the wall and therefore, for our flow tube, the effect of surface recombination was taken into account.

We note from Fig. 4 that in the absence of wall effects, the diffusion term has little effect on the integrated solution. (The solution for $\alpha=0$ can be obtained explicitly without recourse to numerical techniques.)

The radial variation over a cross section at $\lambda=2$ is shown in Fig. 6. It can be seen that any appreciable variation over the cross section occurs only for very small values of α. This same conclusion applies when wall effects are taken into account, as shown in Fig. 7. Here, however, the integrated solution as a function of λ is more dependent on α, as can be seen by comparing Fig. 4 with Fig. 5. The solutions described indicate that volume experiments should be performed with α small. In this way, a radial concentration gradient that will reduce the concentration at the walls and thus minimize surface effects can be established. This means that C_0 and R should be made as large as possible. By increasing R and C_0 the volume recombination is enhanced in other ways, too. Since the volume recombination is second-order in C and surface recombination is first-order, large C_0 will increase the volume effect. Increasing R will increase the volume-to-surface ratio, and thus enhance volume recombination also.

IV. EXPERIMENTAL TECHNIQUES

Side-Arm Experiments

A typical side arm, together with the discharge and detection cavities is shown in Fig. 3. To carry out an experiment, the apparatus that is shown was placed in the gap of an electromagnet so that the magnetic field was perpendicular to the plane of the figure. The detection cavity, which is a part of the spectrometer, was fixed in the center (most homogeneous region) of the magnetic field. Flexible tubing is used for the inlet and outlet of the flow section and flexible coaxial cable feeds the discharge cavity; thus it is possible to slide the side arm through the detection cavity. Hence, atomic

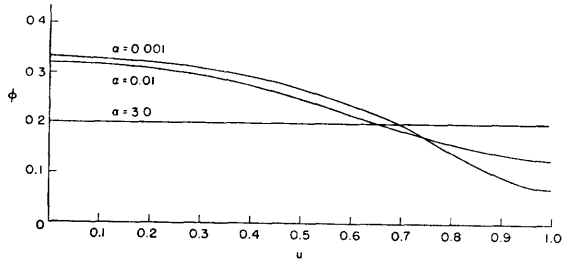

FIG. 6. Calculated ϕ *vs* u at $\lambda=2$ for $(1/\phi)(\partial\phi/\partial u)=0$.

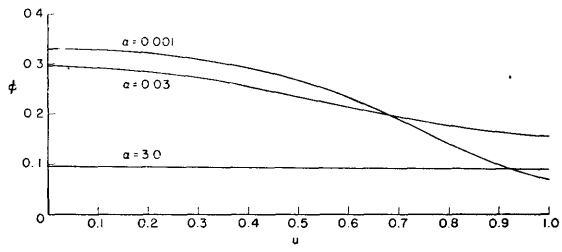

FIG. 7. Calculated ϕ *vs* u at $\lambda=2$ for $(1/\phi)(\partial\phi/\partial u)=-0.05$.

oxygen can be observed as a function of distance along this arm.

The side-arm assembly (except for the joints) was made of quartz, since this material has negligible effect on the cavity Q. Side arms of 1-cm and 0.5-cm diameters were used in this work.

Atomic oxygen was created in the flow stream at the point where it passed through the discharge cavity. (See Appendix A for a discussion on operating a discharge in a magnetic field.) Power for the discharge was obtained from a QK-62 magnetron tuned to the discharge-cavity frequency and operated with a power output of approximately 20 watts. Connection between magnetron and cavity was through $\frac{7}{8}$-in. coaxial cable. The magnetron output power was controlled by varying the bias on a Type 813 tube in series with the magnetron. This current-control method was also used to cut off the discharge when diffusion coefficient measurements were made.

In the diffusion coefficient measurements, the detection cavity and side arm were set at some fixed relative position and the output of the spectrometer was fed into a Tektronix Type 541 oscilloscope. A pulse applied simultaneously to the grid of the Type 813 tube and to the sweep trigger of the Tektronix oscilloscope shut off the discharge and initiated the sweep. No problems were encountered in sustaining the discharge even at the highest pressure in our experiments. However, it was frequently necessary to initiate the discharge with the aid of a Tesla coil.

Flow Experiments

Flow experiments were performed in a quartz flow tube of approximately 1-cm diameter. The flow tube passed through a fixed detection cavity and movable discharge cavity (see Fig. 8). Variable flow distance was achieved by moving the discharge cavity along the flow tube.

Some difficulty was encountered because of heating of the flow tube by the discharge. This was a particular problem in the flow experiments since the heating was of a region in which the observed reaction took place. The effect of such heating was minimized by taking data as the discharge cavity was moved *toward* the detection cavity. In this way, the region that was heated in the discharge is put outside of the reaction area. A stream

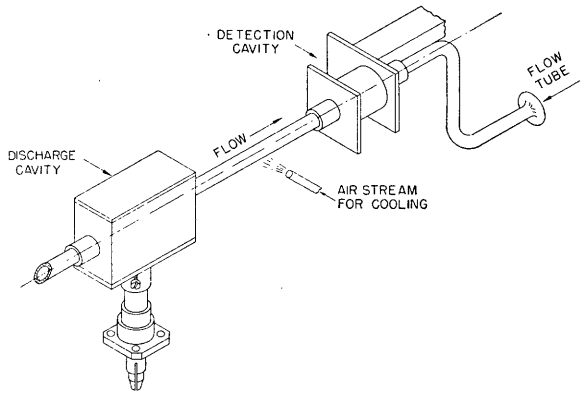

FIG. 8. Detection and discharge cavities for flow method.

of air directed on the quartz tube at the point where it leaves the discharge cavity aided in cooling the reaction region.

Chemical Contamination

The oxygen used in most of the experiments was Airco tank oxygen. Its purity was guaranteed to be 99.5%, with approximately 0.4% argon and 0.1% nitrogen content. The presence of some nitrogen was evidenced by the faint characteristic nitrogen afterglow beyond our discharge. The oxygen was dried by passing it through a dry-ice trap.

Some of our side-arm data were taken with the use of electrolytic oxygen, in which the impurity content was estimated to be less than 0.05 percent. This oxygen was prepared by electrolyzing a solution of potassium hydroxide to which some barium hydroxide had been added to remove any dissolved carbon dioxide.[13] The oxygen was then passed through heated palladium asbestos to catalyze the removal of hydrogen, and then was dried in a dry-ice trap. It was soon seen that surface recombination was not observably affected by the use of the pure oxygen, and further experiments were performed with the tank oxygen. Unfortunately, our oxygen generator did not have sufficient capacity for use in the flow experiments. It might be expected that purity would be a more important factor in volume-recombination studies.

Oxygen was admitted to the reaction region through a metering needle valve. The flow rate could be controlled either by using a second valve between the pump and system to constrict the pumping line or by introducing a leak at that point. By suitable adjustment of the inlet valve and pumping control, a variety of pressures and flow rates could be obtained. In general, the side-arm experiments were run at the maximum flow rate to minimize recombination in the region between the discharge and the side-arm junction.

[13] We thank Professor S. C. Collins of the Department of Mechanical Engineering, MIT, for advice on the production of oxygen.

Connections between the valves and flow tube or side-arm assembly were by Tygon tubing and ground-glass joints. Silicone grease, because of its relatively high chemical inertness, was used in the ground-glass joints. The effect of any reaction between the atomic oxygen and the grease was minimized by having no joints in the immediate vicinity of the observation region.

Pressures were measured by means of an oil manometer attached to the system at a point near the reaction region. Flow rate was measured by a Poisieulle's-law flowmeter,[14] consisting of a capillary tube across which an oil manometer was placed. Pressure and flow measurements probably represent the largest source of experimental error. The accuracy of our pressure measurements was approximately 20 percent. In any application of our techniques to a detailed study of recombination it would be relatively simple to achieve an order-of-magnitude increase in accuracy in pressure and flow measurements by using a McLeod gauge for the former and an accurately calibrated capillary tube for the latter.

To obtain meaningful surface recombination data, it is necessary to start with as pure a surface as possible. Our side arms were cleaned by soaking them for several hours in concentrated nitric acid and continuing this process by similar treatment with concentrated hydrochloric acid.[15] Rinsing was done with demineralized distilled water. This chemical cleaning was followed by vacuum pumping with moderate heating until a pressure of a few microns could be easily maintained. That this treatment was adequate is evidenced by the fact that three different side-arm assemblies gave results that were in agreement.

The Spectrometer

The X-band paramagnetic-resonance apparatus used in this investigation was developed by other workers in this laboratory and it has been fully described.[16–19] Only those aspects of the spectrometer which are of direct concern in our recombination experiments are discussed here in detail.

The basic operation of the spectrometer can be understood by reference to the block diagram of Fig. 9. Microwave power from the 2K25 klystron is reflected from the microwave cavity that encloses the atomic-oxygen sample. The klystron frequency is locked to the

[14] S. Dushman, *Scientific Foundations of Vacuum Techniques* (John Wiley & Sons, Inc., New York, 1948), p. 54.

[15] The chemical cleaning procedure was suggested by Professor W. O. Schumb of the Department of Chemistry, MIT.

[16] Strandberg, Johnson, and Eschbach, Rev. Sci. Instr. **25**, 776 (1954).

[17] Strandberg, Tinkham, Solt, and Davis, Rev. Sci. Instr. **27**, 596 (1956).

[18] M. W. P. Strandberg, *Microwave Spectroscopy* (Methuen and Company, Ltd., London, 1954).

[19] G. J. Wolga, "Microwave resonance study of absorption and hyperfine interactions of F centers in alkali halide crystals," Ph.D. thesis, Department of Physics, MIT, 1957.

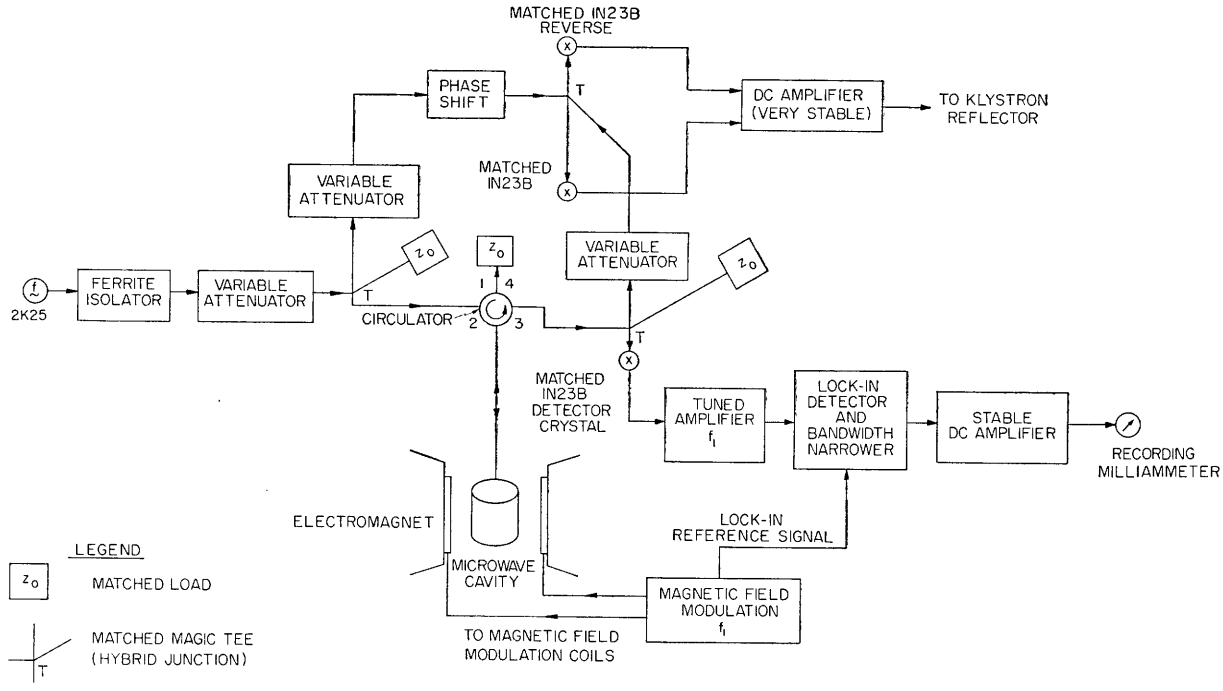

FIG. 9. Paramagnetic-resonance spectrometer.

cavity frequency by means of the discriminator shown in the upper part of the diagram. A 6-kc sinusoidal magnetic field of between 0 and 20 gauss peak-to-peak is superimposed on the dc field of the electromagnet. When the field of the electromagnet is near the resonant field for absorption by the atomic oxygen (approximately 4200 gauss for our cavity frequency), the microwave power reflected from the cavity is modulated at 6 kc with a modulation amplitude that is proportional to the derivative of the absorption-line shape. The 6-kc signal is detected in the 1N23B detector crystal, amplified by the tuned amplifier, and passed through a phase-sensitive detector and band-width-narrowing filter. The output, which then has a greatly enhanced signal-to-noise ratio, is used to drive a recording milliammeter. With a 3-sec time constant on the band-width-narrowing filter, this sytem is capable of detecting absorption by approximately $6\times10^{11}\Delta H$ electron spins per cubic centimeter.

The purpose of our paramagnetic measurements is to determine atomic oxygen concentration at some point along a tube that passes axially through the cavity. However, the cavity has finite length (approximately 4 cm), so that the spectrometer signal measures some average of the concentration over the part of the tube in the cavity. Since the interaction of atomic oxygen with the microwave power is proportional to the *rf* magnetic field, this average is weighted with a factor $\sin^2\pi z/L$ (for a TE_{011} cylindrical cavity), where L is the length of the cavity, and so the observed signal does reasonably represent the concentration at the center of the cavity.

The detection cavity used in this work consists of a glass cylinder coated with a baked thin film of a DuPont glass in silver-paint suspension. The cylinder is clamped between two brass end plates to form the cavity. The use of a silvered cylinder results in having cavity walls sufficiently thin to allow the 6-kc magnetic field modulation to penetrate the cavity without excessive eddy-current losses.

In almost all of our experiments, atomic oxygen was observed by sweeping the dc magnetic field through the resonance and allowing the recorder to trace out the absorption. A typical series of traces as a function of distance down the side arm is shown in Fig. 10. These data can be integrated to obtain absolute concentration (see Appendix B for a method of obtaining $\int\chi''\,dH$ from $d\chi''/dH$), or peak deflections can be compared to obtain relative concentration data. The one exception to the use of the recording milliammeter was in diffusion coefficient measurements. For these measurements, the dc magnetic field was set at the maximum of the derivative, and the output of the tuned amplifier was fed directly to a Tektronix oscilloscope. By cutting off the discharge and triggering the oscilloscope, the decay in concentration as a function of time was presented on the oscilloscope screen and could be photographed.

Presentation of data by means of the recorder has the advantage that the signal has passed through the bandwidth-narrowing filter so that its signal-to-noise ratio is improved, and intensities can be measured more accurately. The absorption, however, must be traced through very slowly (approximately 20 filter time constants, or 3 sec, for RC=0.15 sec) in order to

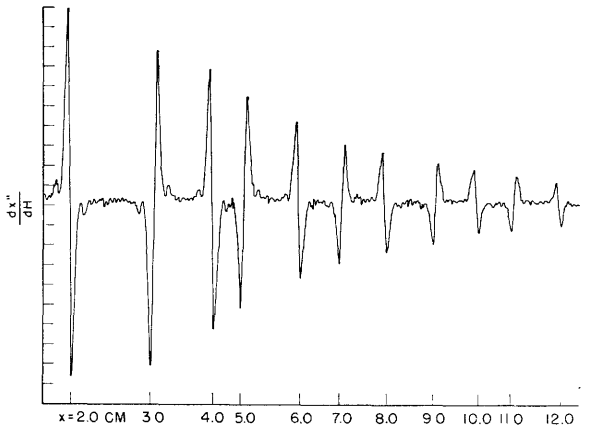

FIG. 10. Typical spectrometer signals at various distances along 1-cm side arm for 1-mm Hg pressure.

achieve faithful reproduction. This restriction limits the recorder tracings to steady-state experiments. It should be pointed out that the amplifier itself is tuned, and hence has a bandwidth that limits the rapidity of observable transient phenomena. This limitation is of the order of several milliseconds. The transient phenomena must have an adequate signal-to-noise ratio to be observable at the amplifier output without additional filtering.

We have mentioned that the output of the spectrometer is proportional to the derivative of the absorption (i.e., to $d\chi''/dH$). This situation is the result of our quasi-static modulation of the applied magnetic field. If we write the field as $H=H_0+H_m\cos\omega_m t$, expand $\chi''(H)$ in terms of $H_m\cos\omega_m t$, and retain only terms in ω_m (which is the only signal passing through the amplifier) for the coefficient of $\cos\omega_m t$, we obtain

$$\chi_1''=H_m(d\chi''/dH)\,|\,H_0+(H_m^3/24)\,(d^3\chi''/dH^3)\,|\,H_0 +\cdots.$$

For sufficiently small values of H_m the filtered signal from the 6-kc amplifier is proportional to $d\chi''/dH$. In actual practice we use a value of H_m which gives us maximum signal. The distortion thus introduced cancels out of our measurements if we keep H_m constant.

It should be apparent, even from the limited treatment of the spectrometer given, that absolute magnitude of the output depends on numerous constants of the apparatus. Some of these, such as rf magnetic field at the sample and crystal conversion gain, are particularly difficult to determine. For this reason, experiments for measuring absolute atomic oxygen concentration were performed by comparing the atomic-oxygen signal with the signal of molecular oxygen with a known pressure filling the same region of the cavity. In this way, all the apparatus constants cancel out.

V. RESULTS

Surface Recombination

Surface-recombination data were obtained by the side-arm method. Logarithmic plots of atomic-oxygen concentration as a function of distance along the side arm for the 1.03-cm diameter side arm are shown in Fig. 11. Figure 12 presents similar data for a side arm of 0.51-cm diameter. It can be seen that the points (except for the lowest pressure) fit a straight line with a spread of approximately 10 percent. The deviation at the low pressure is completely explained by the fact that there is appreciable reflection from the closed end of the tube, and so Eq. (14) must be used.

It should be pointed out that the basic accuracy of the method is much better than is indicated by these data. The data of Figs. 11 and 12 were obtained by making two fairly rapid passes of the magnetic field through the resonant-absorption signal for each value of x. By sweeping through the resonance magnetic field slowly, several times for each point, the observed spread is considerably reduced. A least-square fit to such data should give the slope of the logarithmic plot to a fraction of one percent. This experimental accuracy was verified in a preliminary experiment; but the uncertainty in our pressure measurements did not warrant continued work to that degree of accuracy. Even so, it will be seen that the data for different values of pressure and different side arms are mutually consistent.

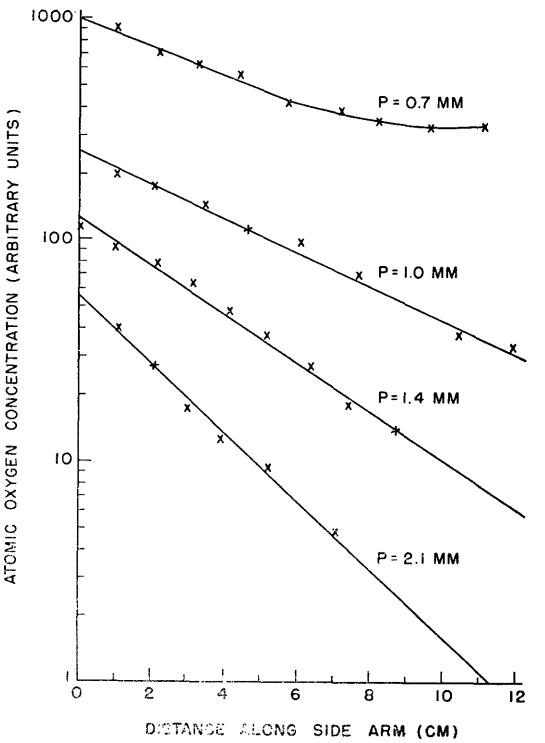

FIG. 11. Atomic oxygen concentration *vs* distance along 1-cm side arm.

The values of α, which are slopes of the logarithmic plots, are shown in Fig. 13, in which their squares are plotted as a function of pressure. Since $\alpha^2=\gamma\bar{v}/2RD$ and D is inversely proportional to p, the plot of Fig. 13 should be a straight line. We note also that α^2 for the 0.5-cm side arm is twice that for the 1-cm side arm, as would be expected for the factor of two difference in the diameters.

All these consistencies indicate that we are observing first-order recombination. As a further check, a few runs were made with reduced atomic-oxygen concentration. If second-order (and also higher-order) recombination is taking place, the logarithmic concentration gradient will, by Eq. (17), be a function of atomic-oxygen concentration. No such change in α with concentration was observed.

That the first-order reaction is a surface recombination and not a volume reaction (e.g., formation of ozone, or oxidation of nitrogen impurities) is proved by the dependence of α on the side-arm diameter. Any volume reaction would give a rate of destruction of atoms proportional to R^2. Since the replenishment of atoms by diffusion is also proportional to R^2, the cross section of the tube cancels out, and such reaction would show no dependence on side-arm size.

The numerical value of recombination efficiency, γ, can be obtained from the slopes of Fig. 13 and from the measured value of Dp. With $\bar{v}$ calculated at 300°K, we obtain $\gamma=3.2\times10^{-4}$. A run taken with moistened oxygen (the oxygen was slowly bubbled through water before being admitted to the side arm) showed no change in γ. We note that our results are consistent with the work of Linnett and Marsden[3,4] on Pyrex.

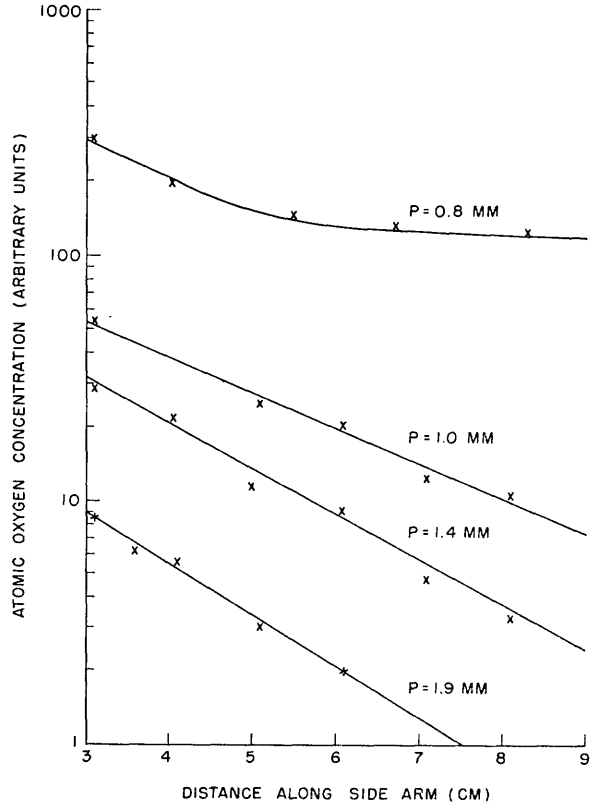

FIG. 12. Atomic oxygen concentration *vs* distance along 0.5-cm side arm.

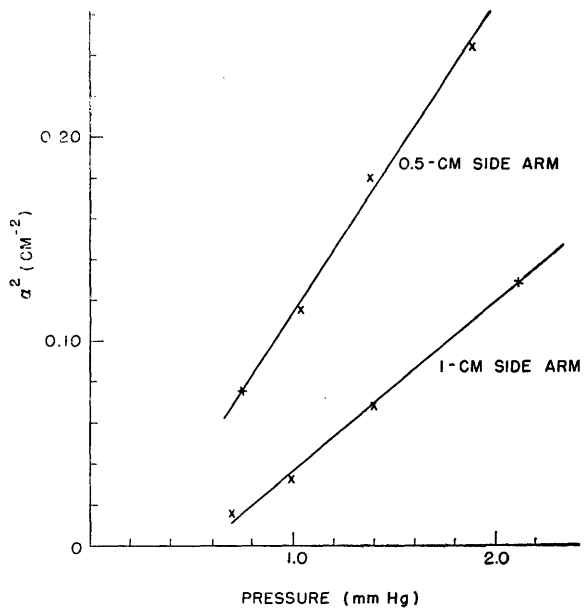

FIG. 13. α^2 *vs* pressure.

Our surface-recombination data indicate unambiguously that the mechanism involved is of first order. This fact excludes any explanation of surface recombination in which two oxygen atoms are required to collide simultaneously at the surface, since this would be a second-order reaction. We look, instead, for a process wherein one atom is already on the surface. Shuler and Laidler[20] have proposed such a mechanism for hydrogen recombination. Their mechanism suggests that a layer of atoms is adsorbed on the surface and that recombination occurs between one of these atoms and an atom striking the surface. Laidler has derived an expression for the recombination efficiency, γ, of such a process which can be evaluated if the activation energy and surface density of oxygen atoms are known. For a slow temperature variation of γ (as observed by Linnett and Marsden), Laidler's expression gives our value of $\gamma=3.2\times10^{-4}$ if the activation energy is 1 kilocalorie gram mole and there are approximately 10^{14} atoms available per square centimeter of surface.

Linnett and Marsden have proposed an alternative mechanism wherein recombination is with one of the oxygen atoms found in the silicates of the quartz. If recombination is to be a first-order process, the surface atoms must be replaced very rapidly. Although the means of replacement is questionable, there is no basic reason to reject this mechanism.

[20] K. E. Shuler and K. J. Laidler, J. Chem. Phys. **17**, 1212 (1949).

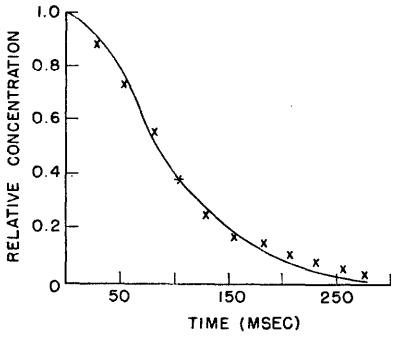

FIG. 14. Atomic-oxygen decay data for $P=1.0$ mm Hg compared with predicted behavior for $D=240$ cm^2/sec.

The processes of Shuler and Laidler and of Linnett and Marsden both involve surface atoms but differ in describing the source of the atoms on the surface. Experimental work over a range of temperatures, surface conditions, and surface materials is necessary to determine the true recombination mechanism. The techniques developed in the work reported here should make it feasible to carry out such a program. The method of making elevated temperature measurements, described by Smith,[2] is directly applicable; low-temperature measurements can also be made by enclosing a portion of the side arm in a cooled jacket. The rapidity with which the data can be obtained simplifies the problem of maintaining a desired surface condition during the course of the experiment. Almost any nonconductive material, even if it is electrically lossy, can be studied by the side-arm technique if it can be deposited in a thin layer. If it is convenient to use material in thicker form, for example, a Pyrex tube, a detection cavity that operates in a higher mode and has a node in the E field at the point where the tube passes through the cavity can be used. Conductive materials might be studied by making the recombining surface part of the cavity wall and observing recombination as a decay of atoms dissociated in the cavity.

The possibility of using paramagnetic-resonance techniques for surface-adsorption studies is also intriguing. We attempted to see oxygen atoms adsorbed on quartz by looking at some quartz wool introduced into one of our sample tubes. Although we did not have any success in this attempt, such investigations might well be continued. We really do not know how fields at the surface perturb the energy levels of the adsorbed atoms or affect the line shape. There is also the question of whether adsorption of a molecule results in dissociation. Such studies might be started with atoms frozen on a surface, since the techniques of low-temperature paramagnetic-resonance studies are well established.

Diffusion Coefficient Measurements

Diffusion coefficients were measured by fitting the observed decay of atomic oxygen when the discharge was turned off to Eq. (20). Figures 14 and 15 show this fit for two values of pressure. The values of Dp thus obtained are 225 cm^2/sec and 240 cm^2/sec. The discrepancy is attributable to uncertainties in pressure measurement, the value of D is in reasonable agreement with values calculated from kinetic theories.[21]

The accuracy of this method of measuring diffusion coefficients can be inferred from Fig. 15 which shows the theoretical behavior for values of D above and below the fitted one. That the predicted D as a function of t drops off faster than the observed data is attributable to the fact that the theoretical calculations assume a sharp cutoff of C_0 at $t=0$, whereas experimentally this drop is spread over approximately 30 msec.

Flow Data

Volume recombination was measured by comparing the atomic oxygen concentration as a function of distance along a flow tube with the calculations plotted in Fig. 5. The data are shown in Fig. 16 which shows relative concentration as a function of distance for various flow rates. All three curves were obtained at a pressure of 5 mm Hg, which was the highest pressure at which we could consistently maintain the discharge. The large pressure was desirable in this experiment because it enhanced volume recombination relative to surface effects.

Comparison of Figs. 5 and 16 indicates that our data do not fit the flow calculation very well. A possible reason for this discrepancy is that commercial Airco tank oxygen was used for these flow experiments. (The oxygen generator that we used to prepare pure oxygen for the surface-recombination experiments could not provide oxygen fast enough for a fast, high-pressure flow.) Both the manufacturer's purity specifications and the presence of an afterglow along the flow line indicated the presence of some nitrogen in the oxygen. Thus, reactions with nitrogen compounds might be responsible for the discrepancy between experimental data and calculations.

Although our calculations do not account for the details of the observed decay, it seems plausible that the concentration decrease is largely caused by oxygen

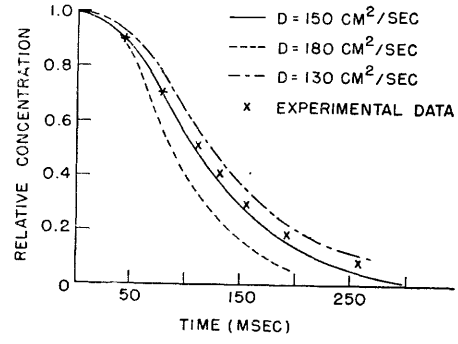

FIG. 15. Atomic-oxygen decay data compared with predicted behavior for $P=1.5$ mm Hg.

[21] W. Jost, *Diffusion in Solids, Liquids, and Gases* (Academic Press, Inc., New York, 1952).

recombination, and so we can still estimate the rate constant, k_2. This was done by noting the distance in which the concentration decreased 75 percent and comparing this distance with the corresponding calculated κ. For the three runs we get an average $\kappa_2 C_0 \approx 35$. If we determined $\kappa_2 C_0$ on the basis of a 50 percent decrease in concentration, we would get $\kappa_2 C_0 \approx 25$. Thus, we obtain an order of magnitude for $\kappa_2 C_0$ from which we can estimate k_2. The third-body concentration, $[M]$, is readily calculated from the known pressure as 25×10^{-8} mole cm^{-3}. C_0 is determined from the absorption signal according to the methods outlined in Sec. II, and is found to be approximately 10 percent or less of the molecular concentration. By using these figures, we get a k_2 of the order of 5×10^{15} cm^6 mole^{-2} sec^{-1}.

The most direct mechanism for volume recombination is a three-body collision involving at least two oxygen atoms. Keck[22] has carried out a theoretical treatment of such a mechanism which indicates that direct three-body recombination is effective only at very high temperatures. He suggests instead that recombination at ordinary temperatures is a two-step process involving the formation of ozone. The reaction mechanism here would be $O+O_2+M \leftrightarrows O_3+M$, coupled with $O+O_3 \rightarrow O_2+O_2$.

The net effect of such a reaction is the same as that of the three-body mechanism. Benson and Axworthy[23] have studied ozone reactions and have determined constants for these processes. The second-order rate constants that can be calculated from the individual reaction rates are lower than our observed rate constant by more than an order of magnitude. In comparing our data with the two-step process it should be borne in mind that Benson and Axworthy's rate constants are for M equal to O_3 rather than O_2.

Our volume-recombination experiments represent an initial effort that can undoubtedly be improved either by modification of the flow scheme or by use of an entirely new approach. As mentioned in Sec. III, volume recombination is favored by making α small. This could be achieved by making the diameter of the flow tube large. The problem of passing the large tube through the cavity can be solved by employing the results of Thompson and Freethy[24] in the design of a cavity with practically no metal at the ends.

The competing surface reaction can also be reduced by "poisoning" the surface. We investigated the effect of Dri-Sil, a General Electric compound that is known to inhibit surface recombination of hydrogen,[25] by coating one of our side arms with this substance. Oxygen recombination was only slightly inhibited by the Dri-Sil; also, the surface became somewhat nonuniform in its recombination properties. Metaphosphoric acid may be a more effective surface inhibitant;[26] if so, it may be possible to use it in conjunction with the side-arm method to obtain volume recombination data by use of Eq. (16) or Eq. (17).

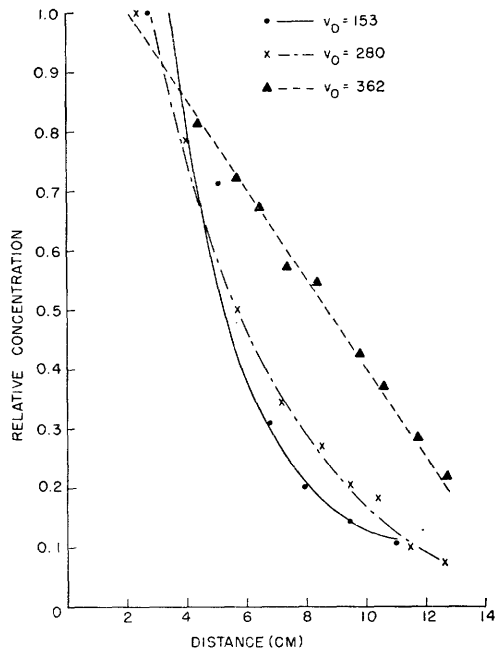

FIG. 16. Relative concentration *vs* distance along flow tube for $P=5$ mm Hg.

Another approach to volume-recombination studies that may be fruitful is to let the cavity be the reaction vessel. Atomic oxygen may be created by a brief discharge, and the concentration as a function of time, after the discharge is turned off, may be used to calculate the recombination constant. The experiment could also be performed by modulating the discharge and relating the recombination constant to the modulation frequency.

The results that we have obtained show that paramagnetic resonance offers a powerful tool for recombination (and other reaction) studies. Applied to atomic oxygen, these techniques have yielded quartz surface-recombination coefficients and volume-recombination data at room temperature. Additional work to further our understanding of recombination phenomena can be conveniently performed by modification of our methods.

APPENDIX A

Operating a Discharge in a Magnetic Field

The fact that our experiments are performed in a magnetic field introduces certain problems in main-

[22] J. Keck, AVCO Research Laboratory, Everett, Massachusetts (private communication).

[23] S. W. Benson and A. E. Axworthy, J. Chem. Phys. **26**, 1718 (1957).

[24] M. C. Thompson, Jr. and F. E. Freethy, "Effect of end-plate modification on Q of X-band cylindrical TE_{011} resonant cavities," National Bureau of Standards, Rept. 5049 Washington, D. C., n. d.

[25] The use of this substance was suggested by the Microwave Gaseous Discharges Group, Research Laboratory of Electronics, MIT, who also made available to us their sample of Dri-Sil.

[26] H. G. Poole, Proc. Roy. Soc. (London) **A163**, 404 (1937).

taining a discharge. In this appendix we point out the aspects of the discharge mechanism that should be taken into account when designing a source for a discharge for recombination experiments. More detailed treatments can be found in the references.[27–29]

In a radiofrequency discharge the electrons are accelerated by the *rf* electric field. Power is abstracted from the electric field because the electrons make collisions with the gas atoms. (A free electron would oscillate with its velocity 90° out of phase with the electric field and could extract no power.) The rate at which an electron acquires energy depends on the *rf* frequency, the collision frequency, and the *rf* field strength.

Breakdown occurs when the rate at which the electrons are produced by ionization balances the rate at which electrons are lost by attachment and by diffusion to the walls. Mathematically,

$$dn/dt=(\nu_i-\nu_a-D/\Lambda^2)n, \tag{A1}$$

where ν_i is the ionization frequency, ν_a is the attachment frequency, D/Λ^2 represents the effect of diffusion of electrons to the walls, Λ represents the characteristic diffusion length and depends upon the geometry of the discharge; for a cylindrical tube $\Lambda=R/2.4$. It is apparent from Eq. (A1) that the discharge will be favored by a large tube. Values of breakdown field for oxygen are given by D. J. Rose and S. C. Brown.[29]

Equation (A1) is complete in the absence of a magnetic field. The effect of a magnetic field on the electrons results in a force equal to $\mathbf{B}\times\mathbf{ev}$, so that the moving electrons are driven into the wall and lost. This loss can be minimized by having the applied electric field parallel to the magnetic field.

In our experiments we used a rectangular TE_{101} cavity through which the tube containing oxygen passed. The cavity was so placed in the magnet gap that the rf electric field inside the cavity was parallel to the applied magnetic field. With this arrangement no difficulty was encountered in maintaining a discharge; also, the use of a cavity (whose Q was approximately 3000) made possible a larger electric field for a given power input.

It is also possible to make a discharge that is self-stabilizing. Since the discharge affects both the Q and the frequency of the cavity by amounts that depend on the intensity of the discharge, the coupling to the cavity can be adjusted so that a change in discharge intensity results in a modification in the cavity fields which, in turn, affects the original discharge variation. Since recombination experiments involve moving the discharge with respect to the magnetic field, a stable discharge is very important.

In some cases (for example, observation of atomic-oxygen decay after the discharge is turned off) it is necessary to know how fast the discharge decays when microwave power is removed. This time can be inferred from Eq. (A1) with $\nu_i=0$. For reasonable geometry, the loss of electrons will be primarily by attachment. Since the attachment frequency, ν_a, for oxygen is of the order of 10^7 per sec, the discharge will decay within a few microseconds.

APPENDIX B

Numerical Integration of Absorption Curves

The paramagnetic-resonance spectrometer presents absorption data as a trace of $d\chi''/dH$ as a function of H. For intensity measurements we require the integral

$$S=\int_0^\infty \chi''dH. \tag{B1}$$

S can be obtained from the experimental data by a single numerical integration as follows. We perform a partial integration on Eq. (B1) to obtain

$$S=[H\chi'']_0^\infty-\int_0^\infty H(d\chi''/dH)dH.$$

In general, χ'' vanishes everywhere except at the resonance. In particular, it is zero at $H=0$ and at $H=\infty$, so that the integral term vanishes. Thus

$$S=-\int_0^\infty H(d\chi''/dH)dH. \tag{B2}$$

For convenience in carrying out numerical integration, we rewrite (B2) as

$$S=-\int_0^\infty (H-H_0)(d\chi''/dH)dH, \tag{B3}$$

where H_0 is the resonant field. S is, of course, unchanged by the introduction of the constant H_0 since

$$\int_0^\infty d\chi''=0.$$

Equation (B2) is independent of line shape and can be applied to our incompletely resolved atomic oxygen transitions.

[27] W. P. Allis, "Motions of ions and electrons," Tech. Rept. 299, Research Laboratory of Electronics, MIT, June 13, 1956.
[28] S. C. Brown, "High-frequency gas-discharge breakdown," Tech. Rept. 301, Research Laboratory of Electronics, MIT, July 25, 1955.
[29] D. J. Rose and S. C. Brown, J. Appl. Phys. **28**, 561 (1957).